Energy landscape steering in SecYEG mediates dynamic coupling in ATP driven protein translocation

Joel A. Crossley,[†,‡,¶] Tomas Fessl,[‡] Matthew A. Watson,[†] Daniel Watkins,[§] Robin A. Corey,[‖] William J. Allen,[§] Tara Sabir,[¶] Sheena E. Radford,[†] Ian Collinson,[*,§] and Roman Tuma[*,†,‡]

†*Astbury Centre for Structural Molecular Biology, School of Molecular and Cellular Biology, Faculty of Biological Sciences, University of Leeds, Leeds, United Kingdom*
‡*Faculty of Science, University of South Bohemia in České Budějovice, České Budějovice, Czech Republic*
¶*School of Clinical and Applied Sciences, Leeds Beckett University, Leeds, United Kingdom*
§*School of Biochemistry, University of Bristol, Bristol, United Kingdom*
‖*Department of Biochemistry, University of Oxford, Oxford, United Kingdom*

E-mail: ian.collinson@bristol.ac.uk; r.tuma@leeds.ac.uk

Abstract

The Sec translocon is a transmembrane assembly highly conserved among all forms of life as the principal route for transport of polypeptides across or into lipid bilayers. In bacteria translocation involves by allosteric communication between the membrane pore SecYEG and the associated SecA ATPase. Using single-molecule fluorescence we reveal that slow conformational changes associated with the ATPase SecA modulate fast opening and closure of the SecY lateral gate. Such mismatch of timescales is not compatible with direct coupling between SecA and SecYEG. A dynamic allosteric model is proposed in which the SecA ATPase cycle 'steers' the energy landscape for SecY pore opening. We map the experimental traces onto reduced reaction coordinates derived from molecular dynamics trajectories, providing a model for the energy landscape and a structural interpretation of the associated dynamics. Dynamic allostery may be common among motor ATPases that drive conformational changes in molecular machines.

Introduction

A fascinating class of biological molecular machines are those operating upon biopolymer substrates and converting chemical energy derived from ATP binding and hydrolysis into cycles of conformational changes and mechanical work (e.g. helicases, translocases, unfoldases, chromatin remodelling complexes and other molecular motors). The bacterial protein secretion system, composed of the integral membrane assembly SecYEG and peripherally associated cytosolic motor ATPase SecA (designated SecYEG:A here), belongs to this class, purposed to translocate unfolded polypeptides across the inner membrane.[1] Secretory proteins (pre-proteins) with N-terminal cleavable signal sequences (SS) are targeted to SecYEG:A for subsequent post-translational transport across the membrane.

In the SecYEG complex, SecY forms the pore for protein translocation (Figure 1A).[1] At the side of the channel is a lateral gate (LG) (Figure 1B).[2] Opening of the LG is required for pre-protein translocation and insertion into

the membrane.[3,4] SecA is a RecA-like ATPase which associates with SecYEG during translocation. It has two nucleotide binding domains forming the ATP binding site.[5] The two-helix finger (2HF) domain of SecA has been proposed to act as a sensor regulating nucleotide exchange,[6,7] or alternatively, to directly push the polypeptide across the membrane.[8,9]

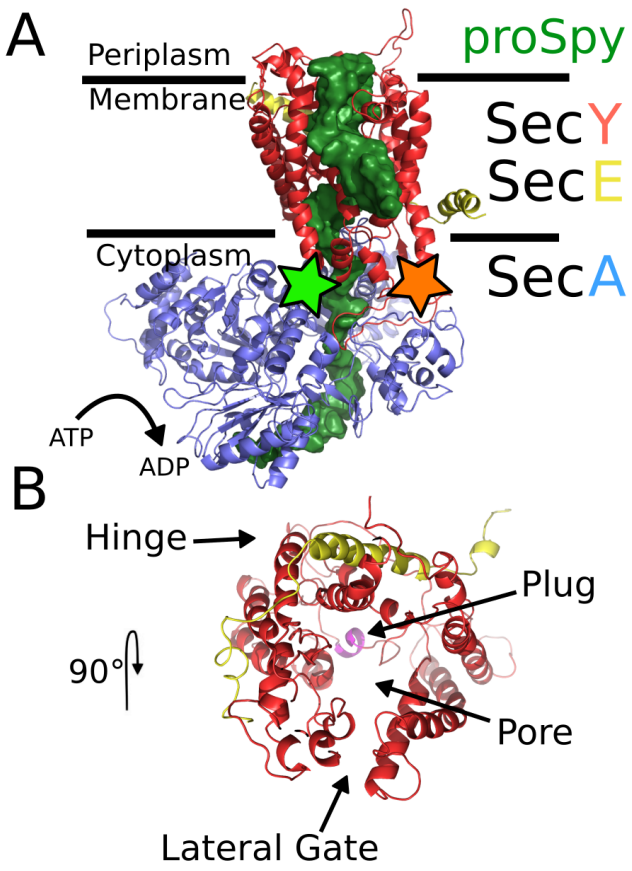

Figure 1: The Structure of Sec translocon. SecY is shown in red, SecE - yellow, SecA - blue, proSpy - Green and Plug in pink. (PDB: 3DIN[10,11]) (A) The structure of SecYEG:A modelled with translocating substrate.[12] Fluorophore placement is shown on the lateral gate in green and orange stars (see Figure S1 for structure based modelling of the dyes). (B) Top down view of SecYEG as seen from the cytoplasm.

The precise nature of the translocation mechanism has divided opinion owing to the inherent complexity of the system.[6,8,9,13] As for other molecular machines which convert the chemical potential of NTP hydrolysis into directional motion, there are two limiting cases of energy transduction: power stroke and Brownian ratchet.[14] The power-stroke mechanism involves deterministic or direct coupling in which each conformation imposed by the stage of the nucleotide hydrolysis cycle is linked with a well-defined conformation of the effector part (e.g. a mechanical lever or substrate binding site) as within a purely mechanical motor. On the other hand, a Brownian ratchet mechanism exhibits loose coupling between the conformations of the nucleotide-binding site of the motor ATPase and the effector part.[15] Both cases can be illustrated in terms of a simplified energy profile along the mechanical reaction coordinate. The power stroke profile features deep minima at either the pre-stroke or post-stroke position which directly correspond to the nucleotide state of the ATPase. In the Brownian ratchet case, the nucleotide-hydrolysis cycle biases a shallow energy profile (i.e. with low energy barriers between states) towards certain conformations which in turn undergo rapid interconversion between the available states due to thermal fluctuations.

The power-stroke mechanism has been demonstrated for many cytoskeletal motors[16] while a Brownian ratchet scheme has been implicated for other ATPases such as the ClpX polypeptide unfoldase.[17] Both mechanisms have been considered for the Sec translocon: the power stroke invokes large, piston-like motion of 2HF imparting force directly to the substrate while SecYEG is considered a passive pore.[8,9] Alternatively, SecY has been proposed to act as Brownian ratchet while allosterically communicating with SecA.[6] A recent single-molecule study detected conformational changes of the 2HF taking place on time scales (measured as dwell times in different states) of 100 - 400 ms,[9] i.e. similar to the timescale of the ATP hydrolysis cycle ($\sim$100 ms),[18] which was interpreted to mean that SecA acts via a directly coupled power stroke. However, in all published structures of the complex[10,11,19,20] there is less than 1 nm available for 2HF movement, and covalent crosslinking of the 2HF to SecY does not prevent translocation activity,[7] suggesting the 2HF does not move much during protein transport. Evidence also points to the SecY pore being actively gated by SecA: (1) opening and closing of the SecY LG is linked to the nucleotide state of

SecA;[6] and (2) rapid relaxation of LG to either open or closed conformation has been observed in molecular dynamics (MD) trajectories in response to changing the identity of the nucleotide bound to SecA from a transition state mimetic (ADP:BeF_x) to ATP or ADP, respectively.[6] Likewise, the nucleotide turnover of SecA is affected by SecYEG: (1) the SecA ATP hydrolysis rate increases ten-fold when complexed to SecYEG and 100-fold during translocation;[18] (2) ADP release is affected by the LG conformation.[6] Further evidence for a two-way dynamic coupling and allostery comes from hydrogen-deuterium exchange experiments.[21]

Understanding dynamic coupling between SecA and SecYEG is key to reconciliation of the apparently distinct mechanisms proposed. The two principle scenarios are considered here: (1) the different conformations of SecYEG (e.g. open and closed states of the channel) deterministically follow the nucleotide state of SecA (2) SecYEG coupling to SecA is stochastic; manifested by rapid interchange between states and controlled by modulations of the underlying energy landscape by the nucleotide status of SecA.

Results

Identification of conformational states of SecYEG Previous structural studies have shown that the LG of SecYEG exhibits three discernible conformational states.[10,14] This was further confirmed by single-molecule fluorescence[6] in which open, part open (here called intermediate) and closed LG conformations were identified, but no transition between these states were previously reported, presumably due to the limited temporal resolution (200 ms per frame) of the total internal reflection fluorescence microscopy (TIRFM). Hence we employed a faster confocal approach (temporal resolution ∼0.1 ms) with the aim to detect and resolve transitions. During the SecA ATPase-coupled translocation of substrate through the translocon, the FRET signal between the dyes acts as a proxy for the the LG conformational state (Figure 1, Figure 2A and Figure S1).

The conditions most relevant to translocation - SecYEG:A alone and SecYEG:A+ADP (both at equilibrium), and SecYEG:A+ATP and SecYEG:A+ATP+substrate (proSpy) (both away from equilibrium), yielded FRET efficiency distributions well-explained by fitting to three populations corresponding to the open, intermediate and closed LG conformational states. This assignment is further supported by modelling fluorophore accessible volumes to distinct species observed by MD[6,12] that yielded three corresponding simulated FRET distributions (Figure S1B).

The relative populations of the different states could be evaluated for samples in the presence of the various nucleotides and soluble periplasmic substrate, proSpy, with FRET efficiency (E_{FRET}) values of 0.25, 0.50 and 0.72, for open, intermediate and closed state, respectively (Figure 2 and Figure S2); all of which were in good qualitative agreement with the previously published TIRFM conducted with an alternative pre-protein (proOmpA) (E_{FRET} ∼0.45, 0.59, and 0.76 for open, intermediate and closed state, respectively).[6] In fact, better time-resolution led to reduced averaging due to rapid state interconversion and helped to discern a shift in the FRET efficiency distribution for the closed state during translocation (from E_{FRET} 0.72 to 0.65, compare panels E and F in Figure S2). Presumably, this reflects SS induced unlocking of SecYEG[22–24] and the presence of substrate precluding complete closure of the gate.

Dynamic behaviour of the SecYEG lateral gate In order to examine the dynamic equilibria of the LG conformational states, and its response to SecA, different nucleotides, and the pre-protein proSpy, we compiled two-dimensional (2D) histograms of FRET efficiency (E) and the corresponding donor lifetime obtained for each burst (τ_D) (Figure 3A-C and Figure S3). Such two-dimensional analysis allows the determination of dynamic behaviour on the millisecond timescale, defined by the average burst duration (i.e. the time it takes for the lipid vesicle to diffuse through the confocal volume; Figure S4 and Figure S5AB). Bursts

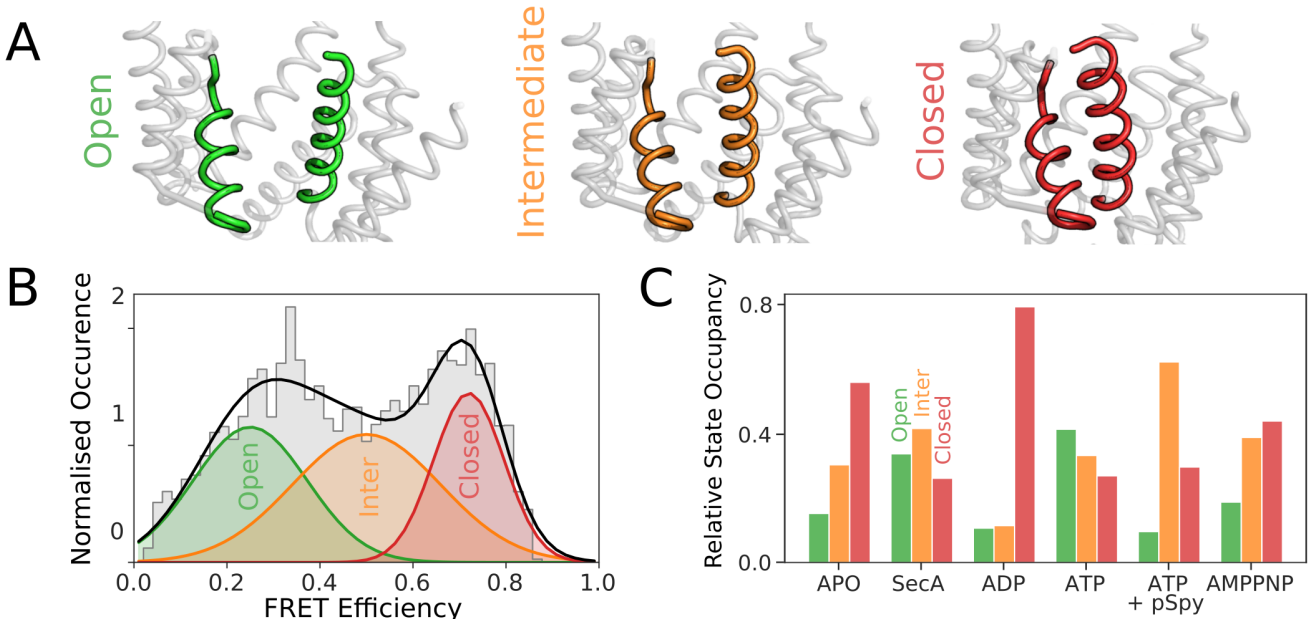

Figure 2: Conformational states of the lateral gate of SecYEG. Green = open, orange = intermediate, red = closed. (A) Side view of helices lining the lateral gate. The open, closed and intermediate states of LG are from representative frames from the equilibrium part of each MD trajectory (basins of attraction in Figure 4A). (B) Representative FRET efficiency histogram for SecYEG:A. Grey bins represent the experimentally observed distribution of E values (corrected for the population of apo SecYEG (unable to bind SecA due to their orientation in the membrane[6]) - Figure S2A) while coloured overlaid Gaussians correspond to the components assigned to the three conformational states. The sum of the Gaussians is shown as a solid black line. (C) The relative population of conformational states of the lateral gate in each experimental condition in Figures 2B and S2A-E.

for which E and τ_D are approximately anticorrelated and fall into the vicinity of the diagonal, 'static line' exhibit no transitions, while those deviating from this line to the right indicate dynamic transitions on the millisecond timescale (for further explanations see Figure S5).

At equilibrium, the LG in both SecYEG alone and SecYEG:A exhibits intrinsic dynamic interconversion between all three states, although the closed state (E_{FRET} = 0.72, τ_D ~1.5 ns) dominates (Figure 3A, Figure S3A and Figure 2C). This interconversion was unexpectedly fast, on the diffusion timescale (represented by the mean burst width 5.75 ms, Figure S4), corresponding to a rate constant of ~175 s^{-1}. Similar dynamic behaviour was observed in SecYEG:A when saturated by AMP-PNP (a non-hydrolysable analogue of ATP) (Figure S3C). However, addition of excess ADP prevents opening of the gate almost entirely, effectively shutting down all dynamics on this timescale (Figure 3B). Interestingly, during conditions of steady state ATP turnover the dynamic behaviour is further accentuated relative to the equilibrium condition, including an increased population of the open state (Figure 3C). As noted above, in the presence of translocating substrate the closed state shifts to lower E_{FRET}.

The presence of FRET events along the 'dynamic line' in the E_{FRET}/τ_D plots suggests that the dynamic transitions occur on a timescale similar to that of diffusion of the proteoliposomes through the confocal volume i.e. a few milliseconds (Figure S5), and thus it should be possible to detect transitions between individual states that occur more rapidly than the diffusion time. Thus, we performed a Hidden Markov Model (HMM) analysis in order to directly detect transitions between states in the real time traces of individual bursts. While HMM assumes that the transitions are essentially instantaneous, most of the detected transitions had a non-zero duration. Hence, we further analysed the identified transitions by fitting a three-segment line to each transition and the flanking regions (Figure 3D). Alignment of the FRET traces at the mid-point ($[t_{start} + t_{end}]/2$) facilitated comparison of char-

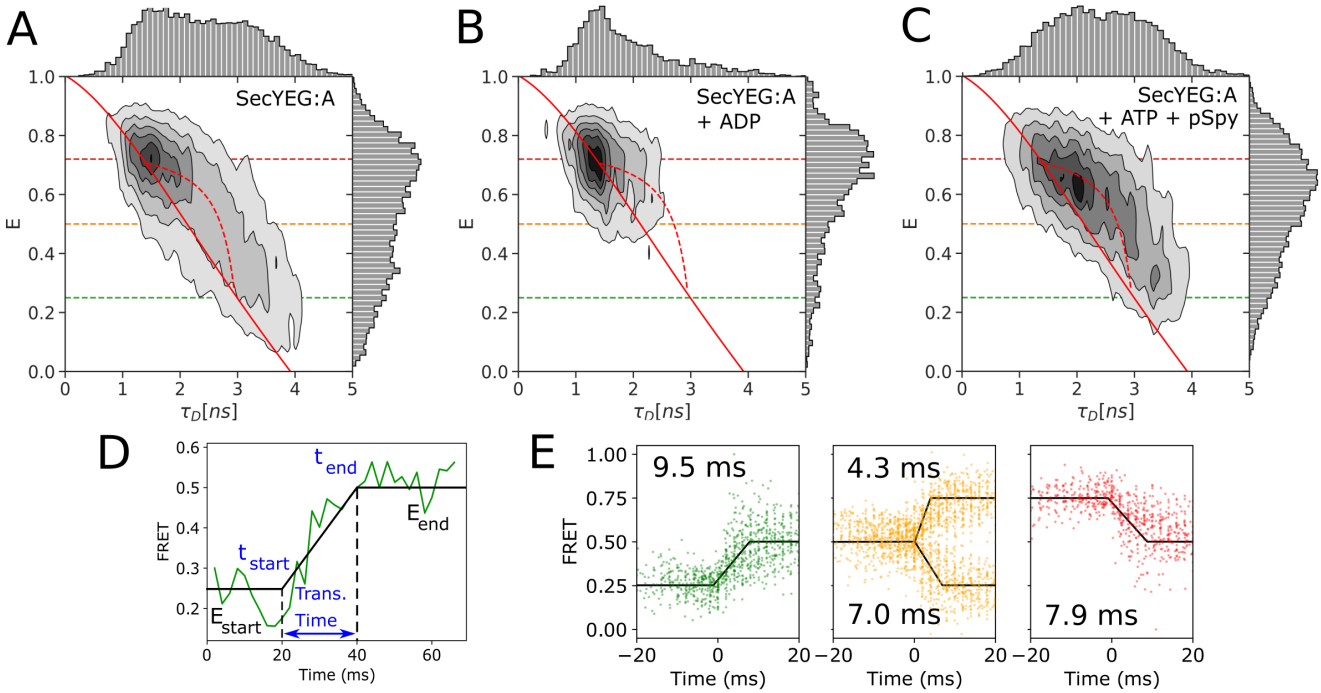

Figure 3: Dynamic behaviour of SecYEG:A LG. Two-dimensional FRET E and donor lifetime (τ_D) analysis for (A) SecYEG:A, (B) SecYEG:A+ADP and (C) SecYEG:A+ATP+proSpy. The solid diagonal and dashed lines represent the static and dynamic fits, respectively (see Figure S5 for details). Horizontal dashed coloured lines indicate the centres of the E_{FRET} values of the closed (red), intermediate (orange) and open (green) lateral gate states. (D) An example of a transition (delineated by dashed vertical lines) from experimental E_{FRET} traces (solid green line) and fitted to a three-segment line (solid black) in order to define start and end times and FRET efficiency values. (E) Transitions in SecYEG:A+ATP. Transitions were aligned using the origin (t_{start}) and classified according to the initial (E_{start}) state. Transitions originating from open are shown in green, intermediate in orange and closed in red.

acteristic time scales for the different transitions under different conditions (Figure 3E and Figure S6). From this representation it is clear that in the presence of ATP the system undergoes dynamic transitions on the millisecond time scale (duration <10 ms, Figure 3E), while in the presence of ADP transitions are rare or longer than the accessible time scale (>50 ms) (Figure S6). The duration of transitions under the conditions of ATP turnover is congruent with the rate estimate 175 s^{-1} made above.

The pattern of transitions in Figure 3E (ATP) suggests that opening and closing occurs via the intermediate state. This is further supported by histograms of transition frequencies obtained from HMM analysis in which direct open to closed and closed to open transitions are relatively rare (Figure S7). Thus, while the intermediate state is only transiently populated, it seems to be an obligatory step along the LG reaction coordinate. The low frequency of 'direct' open to closed transitions also suggests that most transitions can be resolved by our detection system on the millisecond time scale without dynamic averaging.

In summary, the results presented here show that the LG undergoes dynamic transitions on 5-10 ms time scale, which is an order of magnitude faster that the ATPase cycle, as well as the conformational changes of SecA recently observed by single molecule fluorescence.[9,25] However, the average population of the states is clearly linked to the SecA ATPase cycle (Figure 2C) and thus the 'fast' LG opening reaction coordinate must be stochastically coupled to the 'slow' SecA chemical reaction coordinate.

Mapping the lateral gate dynamics onto reduced energy landscape There are now multiple high resolution structures available of the SecYEG:A complex[10,11] as well as MD trajectories exhibiting transitions from the 'high-energy' intermediate SecYEG:A:ADP:BeF_x to structures with open or closed LG.[6,12] There-

fore, we reasoned that they might together contain enough information to give structural insights into the dynamic coupling between SecYEG and SecA through mapping of the experimentally observed dynamics along the LG reaction coordinate onto a reduced set of coordinates that represent the structural changes.

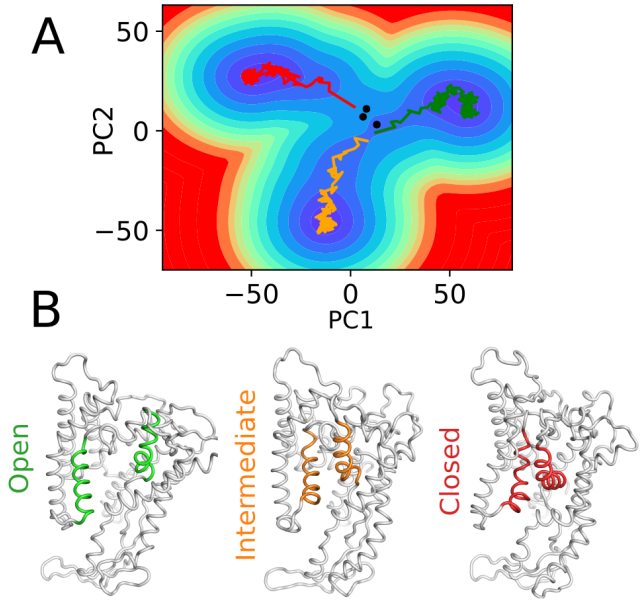

Figure 4: SecYEG:A pseudo energy landscape and associated conformers. (A) Mapping of molecular dynamics trajectories for each nucleotide-bound state (solid lines) onto the two most significant principal components PC1 and PC2, explore the basins associated with the closed (red), intermediate (yellow) and open (green) states. Black dots correspond to the several high-resolution structures (see Methods) which were also included in principle component analysis data set. A pseudo free energy landscape in the background (contours) was computed from the density of molecular dynamics states when projected onto the PC1-PC2 space. (B) SecYEG structures representing the basins of attraction. The lateral gate helices are highlighted in corresponding colors. While PCA analysis recapitulates well the experimentally observed FRET transitions it was performed for a limited number of MD frames and thus is unlikely to describe all changes associated with the ATPase cycle.

To investigate this, we first used invariant core analysis (ICA) to identify parts of the SecYEG structure that undergo structural rearrangements and then projected these changes onto a reduced set of coordinates by PCA (Supporting Information Materials and Methods). ICA identified the two transmembrane helices (TMHs) lining LG (TMHs 2+7, shown in pink and red, respectively in Figure S8) as mobile while these changes were also accompanied by bending of TMHs 4,5+8. Principal component analysis (PCA) enables identification and ranking of structural motions that explain variability across the whole data set. PCA ranking yielded two dominant components which account for 77% variability among the SecY structures (Figure S9). The high-resolution structure, which was used as starting point for MD simulations and corresponds to the 'high-energy' transition state, maps in the middle of the projection space defined by the two dominant principal coordinates (black dots in Figure 4A). Depending on the SecA nucleotide state, MD simulation frames then 'drift' away from this starting point towards three basins of attraction (Figure 4A). As expected, the average potential energy within these basins is lower but comparable for all conditions and fluctuates considerably (Figure S10). FRET efficiencies which were estimated for LG pair for each MD frame quickly reach stable averages (Figure S11) which correspond to the experimentally observed values for open, intermediate and closed states, respectively. The structures representing the three basins (Figure 4B) further illustrate that most of the changes are associated with TMHs lining the LG. However, when the changes are separated according the two PC coordinates (Supplementary Video S1 and Video S2) motion along PC1 is mostly producing LG widening, while PC2 is characterized by sliding of TMHs that line the LG. The 2D representation (Figure 3A) also shows that the intermediate state is reached mostly by progression along the PC2 coordinate. Given that the intermediate state constitutes an obligatory step of LG opening and closing it is necessary to consider both coordinates.

The density of MD states within the reduced 2D representation was used to estimate a probability kernel density which was further converted into pseudo free energy landscape as shown by the contour plot in Figure 4A. Due to the paucity of higher energy states this does not represent a true free energy landscape but provides a convenient backdrop for discussion of the coupling between the chemical reaction

coordinate (ATP turnover) and the fast LG dynamics.

Discussion

The stark difference in timescales between SecYEG LG dynamics (<10 ms) shown here and those of ATP hydrolysis by SecA (>100 ms) demonstrate that SecYEG and SecA cannot be coupled directly and that thermal fluctuations play an important role in the pre-protein translocation mechanism. Indeed, lateral gating by SecY has been shown previously to be strongly dependent on temperature.[26] Rapid dynamic interchange is an intrinsic property of the SecY LG, even in the absence of SecA; although the closed state is the most highly populated state (Figure 3 and 2B). The presence of SecA alone allosterically changes this rapid equilibrium by promoting the open LG conformation (Figure 2C). This allosteric effect further depends on the nucleotide state of the ATPase (Figure 2 and Figure S2). We propose that this is achieved via modulation of the energy landscape associated with LG opening and closing (Figure 5).

We performed PCA on MD simulation trajectories to reduce the dimensionality of the associated landscape and derived a 2D free energy surface and linked the three basins of attraction to the experimentally observed states of the LG (Figure 4). Given that the MD states quickly relax towards the three basins of attraction, this approach has limited sampling of higher energy states, e.g. those close to the saddle points and corresponding transition states. However, by linking the short MD trajectories with experimentally observable FRET values we can estimate the relative depth of the basins (using the steady state populations) as they are being modulated by the nucleotide state of SecA, effectively tilting the energy landscape (Figure 5). Similarly, rapid fluctuations between states suggest that the associated barriers are relatively low, resulting in a shallow landscape.

Figure 5 illustrates 'steering' of SecYEG energy landscape in the context of SecA driven polypeptide translocation. After loading the substrate the ATP state tilts the landscape along the diagonal in favour of dynamic equilibrium between the open and intermediate states and permits substrate diffusion. Upon hydrolysis and phosphate release (ADP state), the landscape tilts towards the closed state, disfavouring dynamics and abrogating polypeptide substrate diffusion. Since ADP release is the rate limiting step of SecA ATPase cycle[18] this constitutes the long lived state and indeed very few transitions are being observed (Figure S6). Upon ADP dissociation, the landscape tilts back to a similar level as seen for the ATP state, perhaps priming the system for rapid rebinding of ATP and also permitting substrate diffusion.

Projection of the overall LG opening onto the reduced principal coordinates (see Video S1 and S2) provides further insight into possible coupling between SecA conformation and SecYEG dynamics. Subtle changes at the cytoplasmic SecA interface, namely repositioning of loop C2 (∼3 Å) and the C-terminal helices TMHs 5-10, lead to an amplification into substantial lateral motion of the LG TMH 7 at the periplasmic side (PC1, Video S1) as well as sliding of TMH 2 with respect to TMH 7 (PC2, Video S2). Both motions lead to an enlargement of the periplasmic cavity in the open state while the cytoplasmic cavity, which is in the vicinity of 2HF and TMHs 6-9, is significantly smaller in the ADP state.[12] This suggests that subtle movements within SecA at the SecYEG interface (e.g. the helical scaffold domain and 2HF) are amplified and leveraged through transmembrane helices leading to large changes in the LG and cytoplasmic and periplasmic cavity sizes.

So why are SecA and SecYEG not directly coupled in a power stroke-like mechanism? Our data and the recent SecA smFRET studies[9,12,27] indicate that SecYEG and SecA operate on separate, but stochastically coupled timescales. Perhaps, while SecA, during its ∼500 ms cycle, can 'grab' the pre-protein substrate and translocate about 20 amino acids (based on ∼40 aa/s processive rate[22]), SecYEG operates on a much shorter time scale of <10 ms, which is less than the average passage time of a single amino acid. Thus, the two machines 'pro-

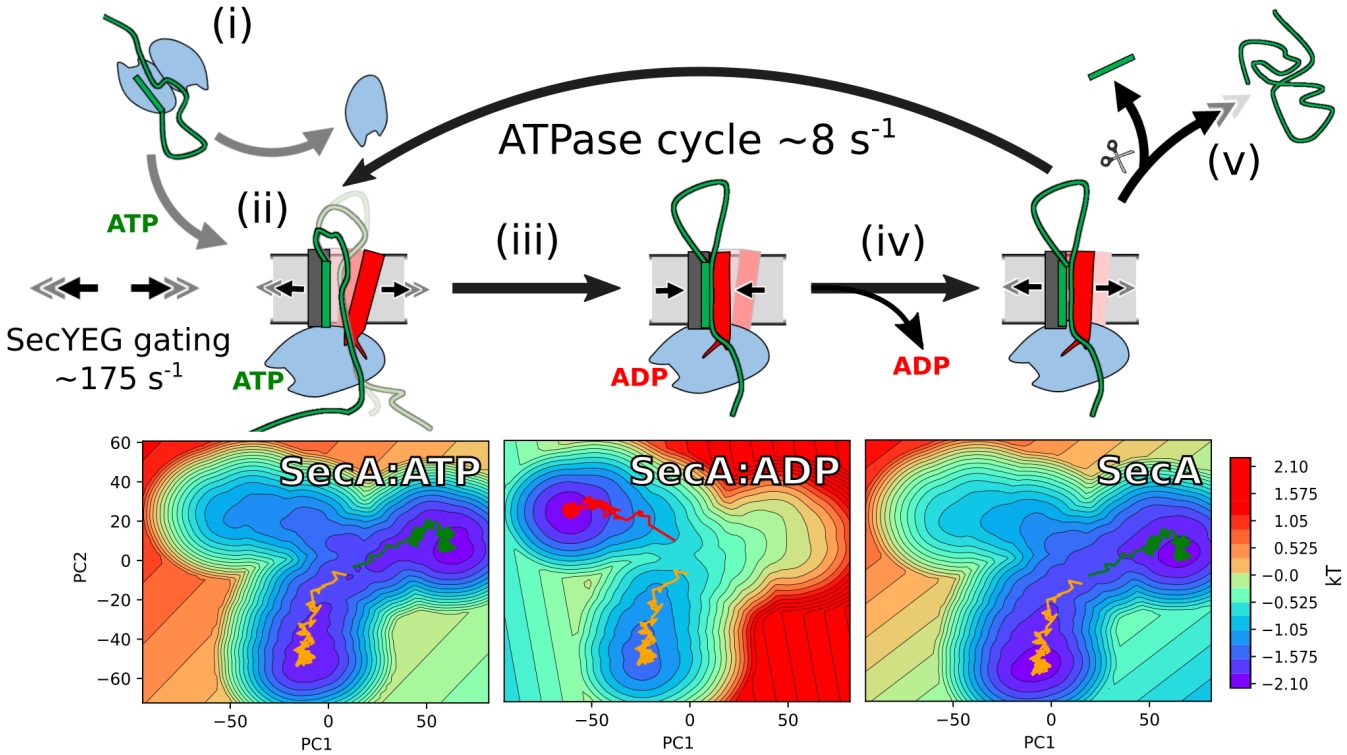

Figure 5: Coupling of the SecYEG LG dynamics to the SecA ATPase cycle via energy landscape steering. (i) The SecA dimer delivers pre-protein to the SecYEG translocon (initiation, see [22]). (ii) In the SecA:ATP state, SecYEG:A steers the energy landscape associated with LG movement (as measured by the E_{FRET} reaction coordinate) to favour the SecY open and intermediate states and rapid interconversion between lateral gate states. (iii) ATP hydrolysis to ADP results in a conformational change in SecA steers the energy landscape to a dominant minimum of the closed state. (iv) ADP dissociation from SecA permits lateral gate dynamics between open and intermediate states. (v) After repeated cycles of ATP hydrolysis, protein translocation is terminated by substrate dissociation and cleavage by signal peptidase, making the overall process irreversible. We used the steady-state population of the three states (Figure 1E) to add realistic tilt (reflected in the colour scale bar) to the two-dimensional landscape. Note that the surface does not represent a true energy landscape that would allow one to make rigorous predictions e.g. about rates and energy barriers.

cess' the translocating polypeptide on different length scales which need to be coupled during translocation. In addition, SecYEG is a versatile machinery, serving in the SecA ATP hydrolysis-driven translocation across the membrane, as well as ribosome GTP hydrolysis-driven co-translational folding into the membrane, with both processes requiring LG dynamics. Since the latter process relies on intimate probing of the lipid environment by the nascent polypeptide chain during initial recognition of the signal anchor and subsequent insertion of TMHs, it may require multiple LG configurations that are readily accessible due to the shallow energy landscape.[4,28,29] Thus, SecYEG may be 'programmed' to exhibit fast LG dynamics which then is further modulated by either SecA in nucleotide-dependent manner, or by the ribosome in a GTP- and nascent chain sequence-dependent manner. We propose that these mechanisms each occur via a general energy landscape biasing, mediated by interactions of SecY cytoplasmic loops with SecA or the ribosome. Such a dynamic allosteric mechanism is not unique to SecYEG:A, since similar nucleotide-dependent steering of rapid dynamics has also been shown recently for adenylate kinase[30] and AAA+ ring ATPase,[30,31] also enabled by advances in single-molecule technology.[32]

Conclusions

We have used time-resolved smFRET combined with analysis of existing crystal structures and

MD simulations to directly observe dynamic interchange between different conformational states of the SecYEG LG. The rates of dynamic exchange between states of the LG are on the order 100-200 s^{-1}, i.e. a time scale at least an order of magnitude faster than the ATPase cycle ($\approx$ 8 s^{-1} in the presence of substrate and $\approx$ 0.3 s^{-1} without[18]). While this observation adds further evidence in support of the two way communication model presented previously,[6] it is clear that the LG opening and closing (i.e. the mechanical reaction coordinate) cannot be directly coupled to the SecA ATPase state (i.e. the chemical reaction coordinate). Thus, even if SecA itself undergoes a power-stroke like cycle, SecYEG LG does not follow it directly state-by-state, but is instead dynamically coupled to SecA conformations.

Dynamic allostery involving motions occurring across multiple time scales coupled via energy landscape bias could be ubiquitous among complex molecular machines. Further experiments exploiting the wide range of timescales and motions now available via smFRET measurements will enable discovery of the extent to which such dynamic allostery is exploited in biology.

Acknowledgement This work was funded by the BBSRC: MAW, RT and SER (BB/N017307/1), DW and IC (BBSRC: BB/N015126/1 and BB/I008675/1), RAC (BBSRC South West Bioscience Doctoral Training Partnership and BB/M003604/I). Additional support was provided by the Wellcome Trust (104632) to IC and ERC ((FP7/2007-2013) / ERC grant agreement 32240) to SER. JC, TF and RT are supported from European Regional Development Fund-Project "Mechanisms and dynamics of macromolecular complexes: from single molecules to cells" (No. CZ.02.1.01/0.0/0.0/15_003/0000441). JC and TS were funded by the School of Clinical and Applied Sciences, Leeds Beckett University.

Supporting Information Available

- Materials and Methods, Supplementary Figures and Description of Videos (.pdf)
- Video S1: SecY projected onto PC1 (.mp4)
- Video S2: SecY projected onto PC2 (.mp4)

References

(1) Brundage, L.; Hendrick, J. P.; Schiebel, E.; Driessen, A. J.; Wickner, W. The purified E. coli integral membrane protein SecY/E is sufficient for reconstitution of SecA-dependent precursor protein translocation. *Cell* **1990**, *62*, 649–57.

(2) Van den Berg, B.; Clemons, J., W. M.; Collinson, I.; Modis, Y.; Hartmann, E.; Harrison, S. C.; Rapoport, T. A. X-ray structure of a protein-conducting channel. *Nature* **2004**, *427*, 36–44.

(3) du Plessis, D. J.; Berrelkamp, G.; Nouwen, N.; Driessen, A. J. The lateral gate of SecYEG opens during protein translocation. *J Biol Chem* **2009**, *284*, 15805–14.

(4) Kater, L.; Frieg, B.; Berninghausen, O.; Gohlke, H.; Beckmann, R.; Kedrov, A. Partially inserted nascent chain unzips the lateral gate of the Sec translocon. *EMBO Rep* **2019**, e48191.

(5) Hunt, J. F.; Weinkauf, S.; Henry, L.; Fak, J. J.; McNicholas, P.; Oliver, D. B.; Deisenhofer, J. Nucleotide control of interdomain interactions in the conformational reaction cycle of SecA. *Science* **2002**, *297*, 2018–26.

(6) Allen, W. J.; Corey, R. A.; Oatley, P.; Sessions, R. B.; Baldwin, S. A.; Radford, S. E.; Tuma, R.; Collinson, I. Two-way communication between SecY and SecA suggests a Brownian ratchet mechanism for protein translocation. *Elife* **2016**, *5*, e15598.

(7) Whitehouse, S.; Gold, V. A.; Robson, A.; Allen, W. J.; Sessions, R. B.; Collinson, I. Mobility of the SecA 2-helix-finger is not essential for polypeptide translocation via the SecYEG complex. *J Cell Biol* **2012**, *199*, 919–29.

(8) Bauer, B. W.; Shemesh, T.; Chen, Y.; Rapoport, T. A. A "push and slide" mechanism allows sequence-insensitive translocation of secretory proteins by the SecA ATPase. *Cell* **2014**, *157*, 1416–29.

(9) Catipovic, M. A.; Bauer, B. W.; Loparo, J. J.; Rapoport, T. A. Protein translocation by the SecA ATPase occurs by a power-stroke mechanism. *EMBO J* **2019**, e101140.

(10) Zimmer, J.; Nam, Y.; Rapoport, T. A. Structure of a complex of the ATPase SecA and the protein-translocation channel. *Nature* **2008**, *455*, 936–43.

(11) Li, L.; Park, E.; Ling, J. J.; Ingram, J.; Ploegh, H.; Rapoport, T. A. Crystal structure of a substrate-engaged SecY protein-translocation channel. *Nature* **2016**, *531*, 395–399.

(12) Corey, R. A.; Ahdash, Z.; Shah, A.; Pyle, E.; Allen, W. J.; Fessl, T.; Lovett, J. E.; Politis, A.; Collinson, I. ATP-induced asymmetric pre-protein folding as a driver of protein translocation through the Sec machinery. *Elife* **2019**, *8*, e41803.

(13) Collinson, I. The Dynamic ATP-Driven Mechanism of Bacterial Protein Translocation and the Critical Role of Phospholipids. *Frontiers in Microbiology* **2019**, *10*, 1217.

(14) Wagoner, J. A.; Dill, K. A. Molecular Motors: Power Strokes Outperform Brownian Ratchets. *Journal of Physical Chemistry B* **2016**, *120*, 6327–6336.

(15) Astumian, R. D. Design principles for Brownian molecular machines: how to swim in molasses and walk in a hurricane. *Physical Chemistry Chemical Physics* **2007**, *9*, 5067–5083.

(16) Lin, J. F.; Okada, K.; Raytchev, M.; Smith, M. C.; Nicastro, D. Structural mechanism of the dynein power stroke. *Nature Cell Biology* **2014**, *16*, 479–U208.

(17) Bell, T. A.; Baker, T. A.; Sauer, R. T. Hinge-Linker Elements in the AAA plus Protein Unfoldase ClpX Mediate Intersubunit Communication, Assembly, and Mechanical Activity. *Biochemistry* **2018**, *57*, 6787–6796.

(18) Robson, A.; Gold, V. A.; Hodson, S.; Clarke, A. R.; Collinson, I. Energy transduction in protein transport and the ATP hydrolytic cycle of SecA. *Proc Natl Acad Sci U S A* **2009**, *106*, 5111–6.

(19) Park, E.; Menetret, J. F.; Gumbart, J. C.; Ludtke, S. J.; Li, W.; Whynot, A.; Rapoport, T. A.; Akey, C. W. Structure of the SecY channel during initiation of protein translocation. *Nature* **2014**, *506*, 102–6.

(20) Ma, C.; Wu, X.; Sun, D.; Park, E.; Catipovic, M. A.; Rapoport, T. A.; Gao, N.; Li, L. Structure of the substrate-engaged SecA-SecY protein translocation machine. *Nat Commun* **2019**, *10*, 2872.

(21) Ahdash, Z.; Pyle, E.; Allen, W.; Corey, R. A.; Collinson, I.; Politis, A. HDX-MS reveals nucleotide-regulated, anti-correlated opening and closure of SecA and SecY channels of the bacterial translocon. *Elife* **2019**, *8*, e47402.

(22) Fessl, T.; Watkins, D.; Oatley, P.; Allen, W. J.; Corey, R. A.; Horne, J.; Baldwin, S. A.; Radford, S. E.; Collinson, I.; Tuma, R. Dynamic action of the Sec machinery during initiation, protein translocation and termination. *Elife* **2018**, *7*, e35112.

(23) Hizlan, D.; Robson, A.; Whitehouse, S.; Gold, V. A.; Vonck, J.; Mills, D.; Kuhlbrandt, W.; Collinson, I. Structure of the SecY complex unlocked by a preprotein mimic. *Cell Rep* **2012**, *1*, 21–8.

(24) Gouridis, G.; Karamanou, S.; Gelis, I.; Kalodimos, C. G.; Economou, A. Signal peptides are allosteric activators of the protein translocase. *Nature* **2009**, *462*, 363–7.

(25) Ernst, I.; Haase, M.; Ernst, S.; Yuan, S.; Kuhn, A.; Leptihn, S. Large conformational changes of a highly dynamic pre-protein binding domain in SecA. *Commun Biol* **2018**, *1*, 130.

(26) Ge, Y.; Draycheva, A.; Bornemann, T.; Rodnina, M. V.; Wintermeyer, W. Lateral opening of the bacterial translocon on ribosome binding and signal peptide insertion. *Nat Commun* **2014**, *5*, 5263.

(27) Chada, N.; Chattrakun, K.; Marsh, B. P.; Mao, C. F.; Bariya, P.; King, G. M. Single-molecule observation of nucleotide induced conformational changes in basal SecA-ATP hydrolysis. *Science Advances* **2018**, *4*.

(28) Bischoff, L.; Wickles, S.; Berninghausen, O.; van der Sluis, E. O.; Beckmann, R. Visualization of a polytopic membrane protein during SecY-mediated membrane insertion. *Nat Commun* **2014**, *5*, 4103.

(29) Wickles, S.; Singharoy, A.; Andreani, J.; Seemayer, S.; Bischoff, L.; Berninghausen, O.; Soeding, J.; Schulten, K.; van der Sluis, E. O.; Beckmann, R. A structural model of the active ribosome-bound membrane protein insertase YidC. *Elife* **2014**, *3*, e03035.

(30) Aviram, H. Y.; Pirchi, M.; Mazal, H.; Barak, Y.; Riven, I.; Haran, G. Direct observation of ultrafast large-scale dynamics of an enzyme under turnover conditions. *Proceedings of the National Academy of Sciences* **2018**, *115*, 3243–3248.

(31) Mazal, H.; Iljina, M.; Barak, Y.; Elad, N.; Rosenzweig, R.; Goloubinoff, P.; Riven, I.; Haran, G. Tunable microsecond dynamics of an allosteric switch regulate the activity of a AAA+ disaggregation machine. *Nat Commun* **2019**, *10*, 1438.

(32) Pirchi, M.; Tsukanov, R.; Khamis, R.; Tomov, T. E.; Berger, Y.; Khara, D. C.; Volkov, H.; Haran, G.; Nir, E. Photon-by-Photon Hidden Markov Model Analysis for Microsecond Single-Molecule FRET Kinetics. *J Phys Chem B* **2016**, *120*, 13065–13075.
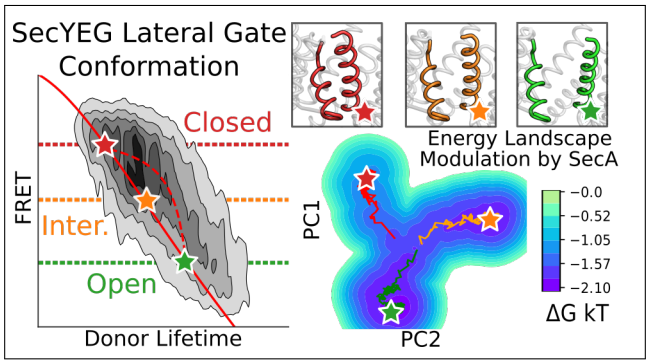
Graphical TOC Entry